TiO2 Pillared Montmorillonite as a Photoactive Adsorbent of Arsenic under UV Irradiation

ARTICLE *in* THE CHEMICAL ENGINEERING JOURNAL · MAY 2012

Impact Factor: 4.32 · DOI: 10.1016/j.cej.2012.02.058

6 AUTHORS, INCLUDING:

Yuan Li
Guangdong Electric Power Design Institute
8 PUBLICATIONS **58** CITATIONS

SEE PROFILE

Chemical Engineering Journal xxx (2012) xxx–xxx

Contents lists available at SciVerse ScienceDirect

Chemical Engineering Journal

journal homepage: www.elsevier.com/locate/cej

TiO_2 pillared montmorillonite as a photoactive adsorbent of arsenic under UV irradiation

Yuan Li [a], Jing Rong Liu [a], Shao Yi Jia [a], Jing Wei Guo [a], Jian Zhuo [b], Ping Na [a,*]

[a] School of Chemical Engineering and Technology, Tianjin University, Tianjin 300072, China
[b] School of Materials Science and Engineering, Hebei University of Technology, Tianjin 300130, China

ARTICLE INFO

Article history:
Received 24 November 2011
Received in revised form 17 February 2012
Accepted 20 February 2012

Keywords:
Titanium dioxide
Pillared montmorillonite
Arsenic
Adsorption
Photocatalysis

ABSTRACT

A TiO_2 pillared montmorillonite (TiO_2/MMT) adsorbent was used to remove As(III) and As(V) from aqueous solution with or without UV irradiation. The adsorption kinetics, role of pH, effect of UV, and column experiments are discussed herein. The Ti-polyoxocations in pillared montmorillonite (MMT) were crystallised to anatase in the interlayer and on the external surface with hydrothermal treatment. The anatase TiO_2 exhibited not only an improved arsenic adsorption capacity, but also enhanced photocatalytic efficiency. The TiO_2/MMT adsorbent was characterised by X-ray diffraction (XRD), transmission electron microscope (TEM), X-ray photo-electron spectroscopy (XPS) and nitrogen adsorption–desorption techniques. The interlayer *d*-spacing and BET-specific surface area increased after intercalation of TiO_2 in montmorillonite. Without UV irradiation, the adsorption capacities of As(III) and As(V) were 4.58 and 4.86 mg g^{-1}. With UV irradiation, the adsorption capacities of As(III) and As(V) were 5.19 and 5.16 mg g^{-1}, respectively, and the equilibrium concentrations of both As(III) and As(V) were below 10 μg L^{-1}. In addition, column experiments of arsenic-contaminated groundwater removal were conducted using granular TiO_2/MMT packed in a 10-cm-ID column with initial arsenic concentrations of 120, 220 and 410 μg L^{-1}. The results indicated that TiO_2/MMT is a promising adsorbent for As(III) and As(V) removal from arsenic-contaminated water.

1. Introduction

High arsenic concentrations in drinking water resource are a major environmental problem and occur in many parts of the world, especially in Bangladesh and West Bengal in India [1,2]. Long-term exposure to arsenic could cause acute and chronic adverse health effects, including cancer [3]. Due to its high toxicity, the World Health Organization (WHO) recommended to lower arsenic levels in drinking water to 10 μg L^{-1} in 1993, and the United States Environmental Protection Agency (US-EPA) published a new 10 μg L^{-1} standard for arsenic levels in drinking water in 2001 [4]. Arsenic is found in a variety of forms in groundwater, including arsenite (As(III)), arsenate (As(V)), methylarsenic (MMA) and dimethylarsenic (DMA), but the main source of arsenic in groundwater is in inorganic forms [5]. Classical technologies such as adsorption, membrane processes, reverse osmosis and ion exchange have been developed to remove arsenic from aqueous systems. Adsorption is one of the most commonly used methods for arsenic removal from aqueous solutions due to its high efficiency and economic value.

Mohan and Pittman compared most of the arsenic adsorbents in a critical review [6]. Iron oxides and activated alumina are the most widespread and effective adsorbents for inorganic arsenic adsorption from aqueous solutions [7,8]. TiO_2 is also an attractive arsenic adsorbent because it is inexpensive and environmentally friendly [9]. TiO_2 nanoparticles are an effective adsorbent for both As(III) and As(V), especially for the adsorption of As(III) under UV irradiation due to its ability to oxidise As(III) to As(V) in the presence of UV light [10–12]. However, the use of TiO_2 nanoparticles is limited to simple applications because the suspensions need to be filtered after the adsorption process. Natural materials, such as kaolinite, montmorillonite and red mud, are used to remove arsenic from water because of their attractive price [13,14]. However, the adsorption capacity of these materials is not satisfactory.

Modified and pillared clays are new possibilities of adsorptive media and are characterised by their favourable microporous structures, economical value and high cation exchange capacity; in addition, these materials are environmentally friendly [15]. The modification of clay is predominantly performed by pillaring various polyoxy cations, such as Al^{3+}, Fe^{3+}, Mn^{4+} and Ti^{4+}. Titania pillared clay has a mesoporous structure due to its small TiO_2 particles acting as pillars between silicate layers, and shows high adsorption ability due to its large specific surface area [16]. TiO_2 pillared montmorillonite has a considerably larger interlayer

* Corresponding author. Tel.: +86 22 27405967; fax: +86 22 27405967.
E-mail address: naping@tju.edu.cn (P. Na).

1385-8947/$ – see front matter © 2012 Elsevier B.V. All rights reserved.
doi:10.1016/j.cej.2012.02.058

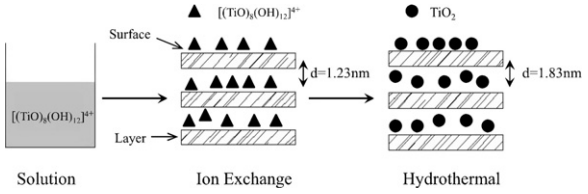

Fig. 1. Schematic diagram for the preparation of TiO_2/MMT.

d-spacing in comparison to other TiO_2 modified clay and shows high adsorption and efficient photocatalytic ability [17,18]. Additionally, the interlayer surface of TiO_2 pillared montmorillonite is generally hydrophobic, which is an advantage in adsorbing and degradation organic compounds in water [19]. Ding et al. reported that TiO_2 pillared montmorillonite showed a high performance for photocatalytic degradation of dimethyl phthalate ester in water [20]. Ooka et al. reported that the hydrothermal treatment TiO_2 pillared montmorillonite could enhance the photocatalytic degradation rate of endocrine disruptors [21]. Furthermore, TiO_2 pillared montmorillonite also show photocatalytic activity owing to nanocrystalline TiO_2 [22]. Thus, this would be one of the suitable materials for the photocatalysis of arsenite in aqueous solution.

The aim of the present work was to prepare TiO_2/MMT by a hydrolysis method and comprehensively evaluate the arsenic adsorption on TiO_2/MMT with and without UV irradiation. After a general characterisation of TiO_2/MMT, the adsorption kinetics data were analysed. The effects of pH and the role of UV light on arsenic adsorption were investigated in order to understand the mechanism of arsenic adsorption under UV irradiation. A column study was carried out to evaluate the application of TiO_2/MMT for arsenic-contaminated groundwater removal.

2. Experimental procedures

2.1. Standards and reagents

All reagents, unless marked in brackets, were purchased from Tianjin Guangfu Fine Chemical Research Institute. All solutions were prepared with analytically pure grade (AR) and deionised water (DI). Na-montmorillonite (MMT) with a cation exchange capacity (CEC) of 0.9 mmol g^{-1} was obtained from Fenghong Corporation (Zhejiang, China). A stock solution of arsenite (1000 mg L^{-1}) was purchased from the Institute of Chemical Reagents (Tianjin, China) and stored under nitrogen until use. Stock solutions of 1000 mg As L^{-1} of arsenic were prepared using sodium salt heptahydrate ($Na_2HAsO_4{\cdot}7H_2O$) (AccuStandard, USA). All labware used in the experiments was soaked in a HNO_3 (7.5 mol L^{-1}) solution for 12 h, washed and then rinsed three times with deionised water.

2.2. Preparation of TiO_2/MMT

The experimental procedure for the preparation of TiO_2/MMT was described in detail by Na et al. [23]. To summarise, TiO_2/MMT was prepared by hydrolysis following a procedure that can be divided into three main steps (Fig. 1). Step 1: preparation of TiO_2 pillared solution: Approximately 100 mL of titanium tetrachloride (Jiangtian Chemical, Tianjin, China) was dissolved in 200 mL of a 3 mol L^{-1} HCl solution under vigorous stirring. The resultant solution was mixed with a 0.5 mol L^{-1} HCl solution in 1:2.5 ratios to form a TiO_2 pillared solution. Step 2: approximately 10 g of Na-montmorillonite was added to 490 mL of deionised water under continuous stirring for 2 h and then was allowed to stand for 12 h at 298 K. Step 3: the TiO_2 pillared solution was added to this mixture and allowed to stir vigorously for 1 h. Next, the mixture was treated in a water bath at 353 K for 6 h. Finally, TiO_2/MMT was separated from the mixture solution and washed several times with deionised water to neutral pH. The wet TiO_2/MMT was then dried in a freeze dryer at 258 K under vacuum. The final TiO_2 content of the TiO_2/MMT was approximately 15.1 wt%.

2.3. Characterisation of TiO_2/MMT

The XRD experiments were carried out using a PANAlytical X-ray diffractometer (PANAlytical Corporation, X'Pert, The Netherlands) with Co Kα radiation (λ = 0.154 nm) 40 kV, 40 mA. The crystal form of TiO_2 in TiO_2/MMT was compared to the XRD patterns of TiO_2.

The electron microscopic investigations and energy dispersive X-ray (EDX) measurements were carried out using a 100 kV transmission electron microscope (TEM), PANAlytical Tecnai G^2 F-20, equipped with an EDX unit (PANAlytical, The Netherlands). The TiO_2/MMT samples were supported on copper mesh with carbon micro-grid.

X-ray photoelectron spectroscopy (XPS) measurements were made using a Physical Electronics PHI 1600 X-ray photoelectron spectrometer (Perkin-Elmer Corporation, USA) with an Mg Kα anode (1253.6 Ev photon energy, 15 kV, 300 W) at a takeoff angle of 45°.

Nitrogen adsorption–desorption isotherms of TiO_2/MMT were obtained at 77 K (Quantachrome Corporation, NOVA-2000, USA). The adsorption and desorption branches of the isotherms were determined. The BET surface area, total pore volume, average pore diameter and pore size distribution curve were calculated from the isotherms. The samples were pretreated in a vacuum (ca. 0.10 Torr) at 423 K for 2 h.

2.4. Arsenic adsorption experiments

Arsenic adsorption experiments were conducted to examine the adsorption behaviour of As(III) and As(V) on TiO_2/MMT. The As(III) or As(V) adsorption experiments were carried out in a 1 L quartz glass vessel, which contained 500 mL of an As(III) or As(V) solution. The solution pH was adjusted with 0.1 mol L^{-1} HCl or 0.1 mol L^{-1} NaOH. After a certain amount of TiO_2/MMT was added, the rotor in a quartz glass vessel was whirled at 150 rpm in a thermostatic batch reactor at 298 K for an appropriate time. In the adsorption kinetics experiments, the As(III) and As(V) solutions with initial concentrations of 5 mg L^{-1} were adjusted to pH 7.0.

2.5. Photoactive adsorption experiments

Photoactive experiments were carried out in a thermostatic batch reactor equipped with a UV lamp (high-pressure mercury lamp, P = 400 W, λ = 240–580 nm, Beijing Lighting Research Institute, China). The distance between the UV lamp and quartz glass vessel was constant during the experiment. In the As(III) adsorption experiments, constant nitrogen purging (10.0 mL min^{-1}) was applied during each irradiation to remove oxygen.

After adsorption, the adsorbent was separated by a filter with a 0.45 μm nylon membrane, and the final As(III) or As(V) concentrations in solution were determined with atomic fluorescence spectrometry (AFS, Beijing Rayleigh, China). The detection limit was determined to be 0.02 μg As L^{-1}.

If necessary, the As(III) and As(V) concentration was determined by AFS after the separation of the arsenic species on a high pressure liquid chromatography (HPLC) system (PRP-X100, Hamilton, Switzerland). The mobile phase was a 20 mM monopotassium phosphate solution, and the solution pH was adjusted to 5.9 with 0.1 mol L^{-1} HCl or 0.1 mol L^{-1} NaOH. The flow rate was 1.0 ml min^{-1}, and the injection volume of sample was 2 μL.

The amount of adsorbed arsenic was calculated from the difference between the initial arsenic concentration and the

Please cite this article in press as: Y. Li, et al., TiO_2 pillared montmorillonite as a photoactive adsorbent of arsenic under UV irradiation, Chem. Eng. J. (2012), doi:10.1016/j.cej.2012.02.058

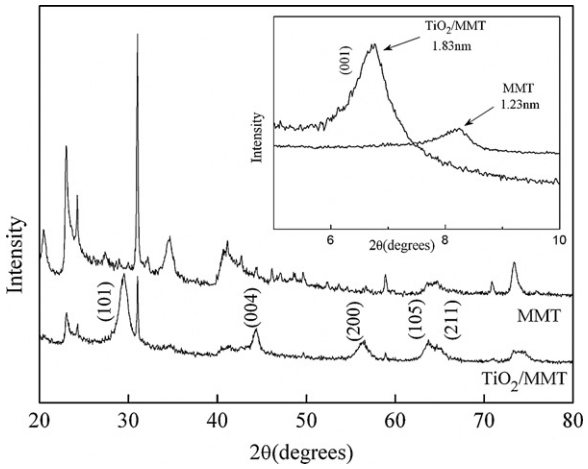

Fig. 2. X-ray diffraction pattern of MMT and TiO_2/MMT.

concentration that remained in the supernatant solution. The adsorption capacity was calculated using the following formula:

$$q_e = \frac{(C_i - C_e)V}{M} \quad (1)$$

where q_e (mg g^{-1}) is the adsorption capacity, C_i (mg L^{-1}) is the initial concentration of arsenic in solution, C_e (mg L^{-1}) is the equilibrium concentration of arsenic in the supernatant, V (L) is the volume of the solution and M (g) is the weight of the TiO_2/MMT adsorbent.

2.6. Column study

A column study was performed to investigate the use of TiO_2/MMT as an effective treatment technology for arsenic removal. Column experiments were conducted in a column (1.0 cm × 10 cm) packed with 3.686 g of granular TiO_2/MMT (0.27–0.55 mm) at 298 K. To investigate the adsorption capacity of TiO_2/MMT, the influent solution contained arsenic-contaminated groundwater from Sanin country (Shanxi, China). Different concentrations of an arsenic solution (pH 8.0 or 8.2) were passed through the column at a flow rate of 5 mL min^{-1}. The concentrations of arsenic were 120 μg L^{-1}, 220 μg L^{-1} and 410 μg L^{-1}. The effluent from the column was collected at regular intervals, and the residual arsenic concentrations were analysed with AFS. The volume at which the arsenic concentration in the effluent reached the maximum permissible value (10 μg L^{-1}) was regarded as the breakthrough point.

3. Results and discussion

3.1. Structure characterisation of TiO_2/MMT

Fig. 2 shows the X-ray diffraction pattern of MMT and TiO_2/MMT. When the TiO_2 was pillared in MMT, obvious peaks at 29.5°, 44.2°, 56.5°, 63.5° and 65.0° were observed. The peak positions and their relative intensities are consistent with the standard powder diffraction pattern of anatase and correspond to the (1 0 1), (0 0 4), (2 0 0), (1 0 5) and (2 1 1) reflections of the crystalline anatase (TiO_2), respectively [24]. Only anatase phases were present, and no rutile phase existed. These anatase phases can more significantly improve the performance of photocatalysis than the rutile phases [25]. The interlayer d-spacing was calculated from the (0 0 1) reflection via the Bragg equation:

$$d = \frac{\lambda}{2 \sin \theta} \quad (2)$$

where λ is the average wavelength of the X-ray radiation and θ is the diffracting angle.

The basal spacing along the [0 0 1] direction (d-spacing) for the MMT was 1.23 nm as shown by the low-angle XRD pattern (small picture in Fig. 2). After pillaring of the MMT particles with TiO_2, the d-spacing increased to 1.83 nm. The shift in the 2θ value also indicated that TiO_2/MMT can increase the d-spacing. This behaviour was similar to that reported for titanium pillared montmorillonite clays [26].

The intercalation of the Ti-polyoxocations into the interlayer of MMT destroyed the ordered structure of MMT to some extent, resulting in some exfoliated one-layer and multilayer sheets, as shown in Fig. 3a and b. This behaviour was similar to that reported for TiO_2 pillared montmorillonite [22]. The Ti-polyoxocations could be adsorbed on the outer surface of the exfoliated silicate layers by the hydrothermal treatment. Therefore, TiO_2 nanoparticles were formed in the interlayer of MMT and on the surface of MMT during the hydrolysis process of the TiO_2/MMT. The image in Fig. 3c shows that the lattice fringe spacing of the anatase TiO_2 nanoparticles, and that some of them are marked by arrows in Fig. 3c. EDX measurement reveals that the TiO_2/MMT contains O, Mg, Al, Si and Ti (Fig. 3d), which is also an evidence that TiO_2 nanoparticles were formed in the interlayer and on the surface of MMT. The Cu was observed, because the sample was placed on copper mesh.

The XPS spectra demonstrate the sensitivity for identifying elements on the surface. The high-resolution utility scans were then used to measure the atomic concentrations of Al, Si, C, Ti and O in the sample (Table 1). Fig. 4 shows the peak positions of carbon, silicon, oxygen, aluminium and titanium obtained by XPS for MMT and TiO_2/MMT. As shown in Fig. 4, the C-1s peak was observed at 288.0 eV due to the widespread presence of carbon in the environment. The TiO_2/MMT sample contained three O-1s peaks positioned at 529.8 eV (20.68%), 531.8 eV (16.81%) and 532.8 eV (62.51%), which were assigned to lattice oxygen O_2^-, bridging OH and adsorbed H_2O, respectively [27]. The Ti-2p peak for TiO_2/MMT was found at 462.4 eV, which can be attributed to the TiO_2 groups in MMT and is in agreement with the XRD and TEM/EDX analysis.

Table 1 shows the structural parameters of MMT and TiO_2/MMT. The specific surface areas of MMT and TiO_2/MMT were 23.7 and 176.4 m^2 g^{-1}, respectively. These values were similar to those reported for TiO_2 pillared MMT [21]. Fig. 5 shows adsorption–desorption isotherms of nitrogen on MMT and TiO_2/MMT. The TiO_2/MMT isotherm seems to be nearly a type IV isotherm (BDDT classification) [19]. Both MMT and TiO_2/MMT loops are similar to the B-type loop, indicating that the formation of these medium-size pores is closely related to the layer structure of montmorillonite [28]. After determining the isotherms, the pore size distribution was calculated from the appropriate section of the desorption branch of each isotherm using the Barrett–Joyner–Halenda (BJH) method [29]. Fig. 6 shows the pore size distribution curves calculated from the isotherms in Fig. 5. It is evident that TiO_2/MMT has a mesoporous structure with a multi-peak distribution, which is mainly a trimodal distribution. There are two types of TiO_2/MMT pores: a two-dimensional pore formed by pillared interlayers and a 'house-of-cards' structure shaped by stacking of the montmorillonite layers. These results indicated that the pore size in TiO_2/MMT increased with hydrothermal treatment. More detailed data are presented in Table 1.

3.2. Adsorption kinetics

The TiO_2/MMT adsorbent was used to remove As(III) and As(V) from an aqueous solution with or without UV irradiation. The kinetics for arsenic adsorption by TiO_2/MMT in the absence and presence of UV light are presented in Figs. 7 and 8. Fig. 7 shows the

Please cite this article in press as: Y. Li, et al., TiO_2 pillared montmorillonite as a photoactive adsorbent of arsenic under UV irradiation, Chem. Eng. J. (2012), doi:10.1016/j.cej.2012.02.058

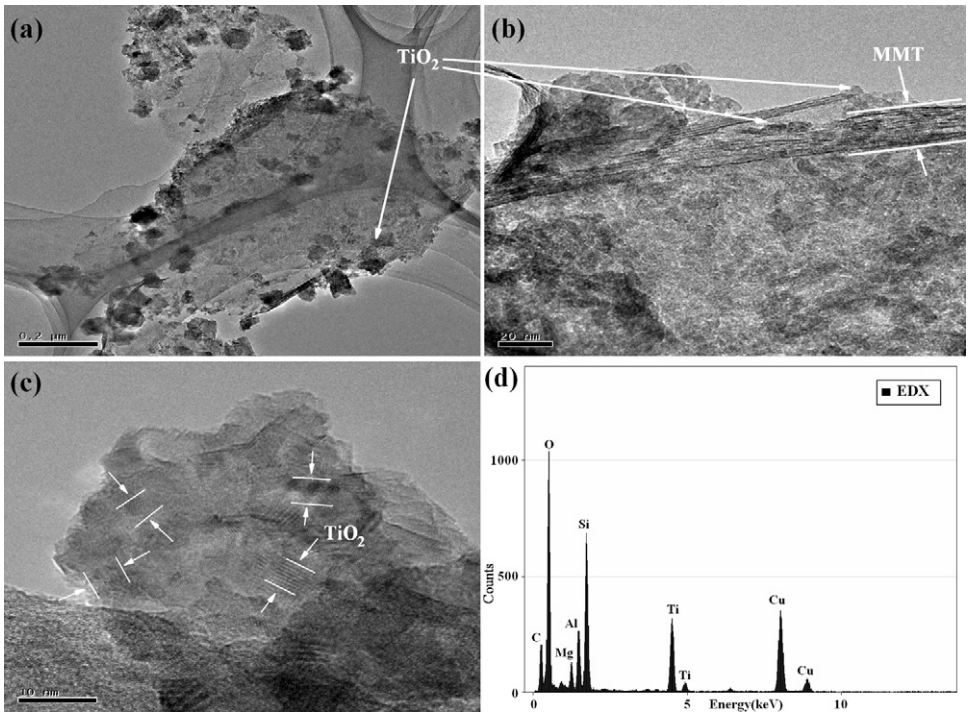

Fig. 3. TEM photographs and EDX pattern of TiO_2/MMT.

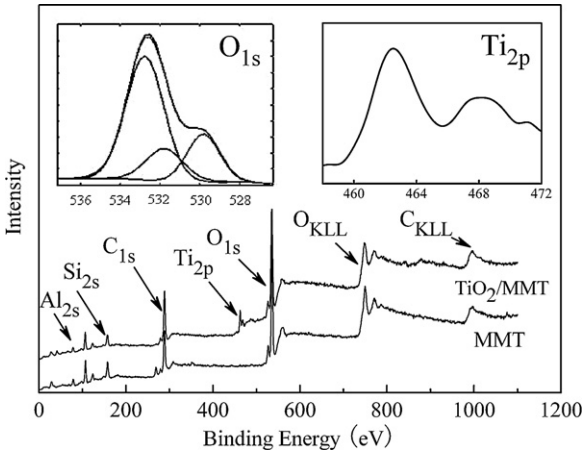

Fig. 4. XPS spectrum of MMT and TiO_2/MMT.

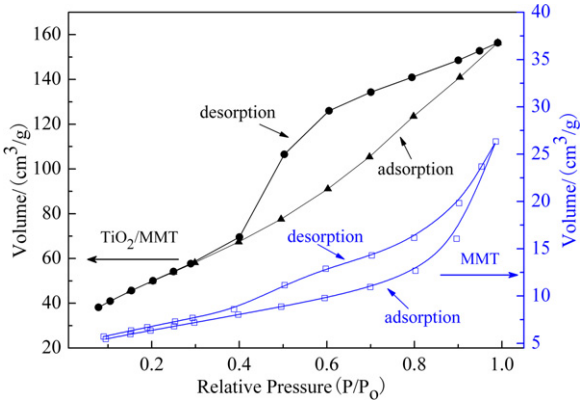

Fig. 5. Adsorption–desorption isotherms of nitrogen on MMT and TiO_2/MMT.

adsorption kinetics of As(III) with initial concentrations of 5 mg L^{-1}. The maximum adsorption capacity increased from 4.58 to 5.19 mg g^{-1} with UV irradiation. The adsorption capacity increased quickly within the first 20 min, and the adsorption equilibrium was less than 1 h. The rapid adsorption in the beginning can be attributed to the greater concentration gradient and to more available sites for adsorption [30]. The adsorption rate in this study is different from published rates using other adsorption processes [31,32]. With UV irradiation, more than 90% of the As(III) was adsorbed in the first 10 min, and equilibrium was reached after approximately 50 min. Fig. 8 shows the adsorption kinetics of As(V) with and without UV irradiation. The results are similar to the adsorption kinetics of As(III), but the effect of UV on As(V) adsorption was not as significant as on As(III) adsorption. Goldberg [33] reported that the adsorption capacities of As(III) and As(V) were

Table 1
Characterisation of MMT and TiO_2/MMT.

Sample	Surface atomic concentrations[a] (%)					Structural parameters			
	C	O	Si	Al	Ti	Surface area[b] (m^2 g^{-1})	Pore diameter[c] (Å)	Pore volume[c] (cm^3 g^{-1})	*d*-Spacing[d] (nm)
MMT	36.1	43.5	13.4	5.1	0	23.70	27.81	0.042	1.23
TiO_2/MMT	42.2	38.8	6.9	3.5	5.6	176.40	28.96	0.23	1.83

[a] Surface atomic concentrations determined by XPS.
[b] BET surface area measured by N_2 adsorption–desorption at liquid N_2 temperature.
[c] Average pore diameter and pore volume obtained from the BJH equation.
[d] *d*-Spacing calculated via $d = \lambda/2 \sin\theta$ from XRD.

Please cite this article in press as: Y. Li, et al., TiO_2 pillared montmorillonite as a photoactive adsorbent of arsenic under UV irradiation, Chem. Eng. J. (2012), doi:10.1016/j.cej.2012.02.058

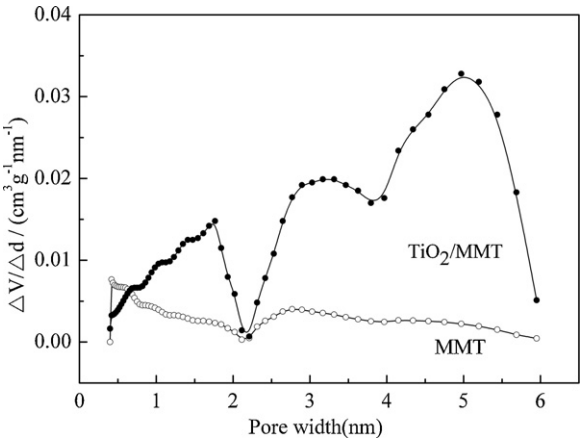

Fig. 6. Pore size distribution curves of MMT and TiO_2/MMT.

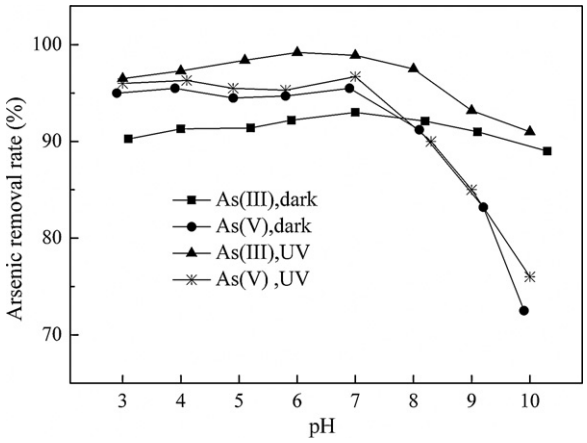

Fig. 9. Effect of pH on arsenic adsorption on TiO_2/MMT with and without UV irradiation.

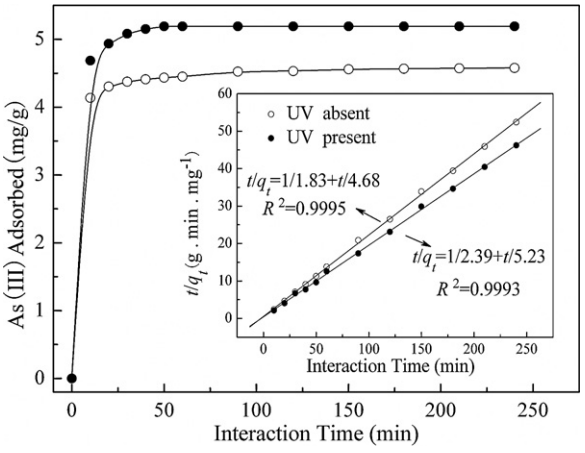

Fig. 7. Kinetics for TiO_2/MMT adsorption of As(III) with and without UV irradiation.

0.32 μmol g^{-1} (equal to 24.0 μg g^{-1}) and 0.22 mmol kg^{-1} (equal to 16.5 μg g^{-1}) for MMT, respectively. Our study confirmed that pillaring TiO_2 into MMT could significantly increase the As(III) and As(V) adsorption capacities of TiO_2/MMT.

To further understand the adsorption kinetics, a pseudo-second-order model, which has been successfully used in many adsorption processes, was selected to fit the adsorption kinetic data [34,35]. The pseudo-second-order model [36] can be expressed as follows:

$$\frac{dq_t}{dt} = k_2(q_e - q_t)^2 \quad (3)$$

$$\frac{t}{q_t} = \frac{1}{k_2 q_t^2} + \frac{t}{q_e} \quad (4)$$

where q_t (mg g^{-1}) is the amount of As adsorbed at time t (min) and q_e (mg g^{-1}) is the amount of adsorption at equilibrium. k_2 (mg g^{-1} min^{-1}) is the pseudo-second-order reaction rate. The parameters k_2 and q_e can be estimated from the intercept and slope of the (t/q_t) vs. t plot, respectively.

As shown in Figs. 7 and 8, the pseudo-second-order model fit the adsorption of As(III) and As(V) on TiO_2/MMT well over the entire adsorption time, as indicated by the high correlation coefficient (R^2). As shown in Fig. 7 (small picture), the equilibrium adsorption amounts of As (III) were 4.68 and 5.23 mg g^{-1} with and without UV, respectively. The initial adsorption rate with UV irradiation (2.39 mg g^{-1} min^{-1}) was higher than that without UV irradiation (1.83 mg g^{-1} min^{-1}), indicating the faster adsorption of As(III) with UV irradiation. The small picture in Fig. 8 shows the pseudo-second-order model curve of As(V) with and without UV irradiation. These results are similar to those of As(III).

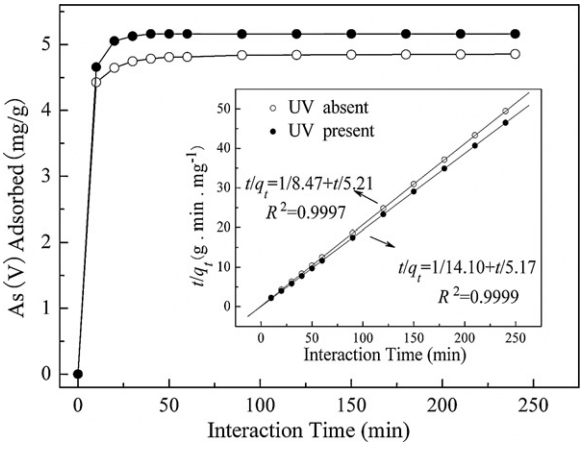

Fig. 8. Kinetics for TiO_2/MMT adsorption of As(V) with and without UV irradiation.

3.3. Effect of pH

It is well known that pH is a critical parameter in arsenic adsorption by TiO_2 and other adsorbents [10,37]. Therefore, the effect of pH on arsenic removal with the TiO_2/MMT adsorbent was investigated using 500 mL of an As(III) or As(V) solution containing an initial arsenic concentration of 5 mg L^{-1}. The solution pH was adjusted with 0.1 mol L^{-1} HCl or 0.1 mol L^{-1} NaOH to obtain pH values ranging from 3 to 10. Higher pH values were avoided because the alkaline environment could lead to partial dissolution of MMT and destabilise TiO_2/MMT. Fig. 9 shows the effect of pH on the As(III) and As(V) adsorption onto TiO_2/MMT with and without UV irradiation. The adsorption behaviours were completely different. Without UV irradiation, the removal rate of As(III) on TiO_2/MMT first increased and then decreased with increasing solution pH. By contrast, the removal rate of As(V) was high and stable at pH values from 2.9 to 7.1, but decreased rapidly when the solution pH increased from 7.1 to 9.9. Other adsorbents such as TiO_2 and modified montmorillonite have also been reported to have low adsorption capacities for As(V) under alkaline conditions [10,14,38]. With UV irradiation, the effect of pH on arsenic adsorption on TiO_2/MMT was similar to that in dark conditions, but the

Please cite this article in press as: Y. Li, et al., TiO_2 pillared montmorillonite as a photoactive adsorbent of arsenic under UV irradiation, Chem. Eng. J. (2012), doi:10.1016/j.cej.2012.02.058

Table 2
The effect of UV light on arsenic adsorption.

Sorbates	Absorbents	Adsorption process	Equilibrium concentration ($\mu g\,L^{-1}$)	Removal rate (%)
As(III)	TiO_2/MMT	Dark	254.0	94.58
	TiO_2/MMT	UV	0	100
	UV irradiation TiO_2/MMT	Dark	120.2	97.71
As(V)	TiO_2/MMT	Dark	70.4	98.56
	TiO_2/MMT	UV	4.0	99.93
	UV irradiation TiO_2/MMT	Dark	17.7	99.65

arsenic removal rate was higher than in the dark. These results are consistent with the adsorption of arsenic other adsorbents with UV irradiation from other studies [32,39]. It is well established that the effect of pH on arsenic adsorption is related to the adsorbent surface charge and the arsenic species [40,41]. As previously discussed, the As(III) species exist in the form of H_3AsO_3 at pH values from 3.0 to 8.0, so a shift in the pH value would have little effect on the adsorption of As(III). However, at pH values from 3.0 to 10.0, As(V) species are present as H_3AsO_4, $H_2AsO_4^-$, and $HAsO_4^{2-}$, which could explain why the adsorption capacity of As(V) varies strongly with pH.

3.4. Effect of UV light

In almost all of the published arsenic adsorption experiments, UV light was present during the adsorption process. However, we found that the arsenic adsorption capacity of the TiO_2/MMT sample was increased with UV irradiation for 2 h before adsorption. To better understand the effect of UV light on arsenic adsorption, a series of experiment were carried out. Three sets of comparative experiments were performed on both As(III) and As(V): TiO_2/MMT adsorption in dark, TiO_2/MMT adsorption with UV irradiation and TiO_2/MMT with UV irradiation for 2 h and adsorption in the dark. To study the effect of UV on the arsenic adsorption experiments, the initial concentrations of As(III) and As(V) were 5 $mg\,L^{-1}$ and the interaction time was 250 min. Table 2 lists the equilibrium concentrations and removal rates of arsenic adsorption with or without UV irradiation. With UV irradiation of TiO_2/MMT the removal rate of As(III) and As(V) increased from 94.58% to 97.71% and from 98.56% to 99.65%, respectively. In the presence of UV radiation, the equilibrium concentrations of As(III) and As(V) were less than 10 $\mu g\,L^{-1}$, which is below the maximum allowable values in drinking water.

The changes of arsenic concentration with an initial As(III) concentration of 5.0 $mg\,L^{-1}$ are summarised in Fig. 10. The left *Y*-axis data shows the As(III) concentration changes after three different treatments. With only UV illumination, not much difference was observed on the concentration of As(III). This result suggests that not much As(III) could be oxidised with UV light alone. Although TiO_2/MMT possess a good adsorption capability on As(III), the remaining As(III) concentration after 150 min adsorption was still at 254.0 $\mu g\,L^{-1}$. With both TiO_2/MMT and UV light illumination, the adsorption of As(III) onto TiO_2/MMT still played the major role. But after 150 min UV light illumination, the remaining As(III) concentration was at 4.0 $\mu g\,L^{-1}$, which represents another degree of decrease over the pure adsorption effect and is lower than the 10 $\mu g\,L^{-1}$ limit.

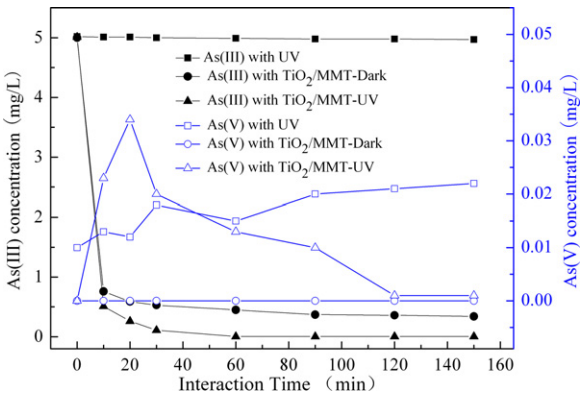

Fig. 10. Arsenic species concentrations vs. treatment time under various conditions.

The right *Y*-axis data in Fig. 10 shows the changes of As(V) concentration under these three treatments in details, respectively. Under only UV light illumination, the As(V) concentration showed a slight increase due to the As(III) oxidation. When TiO_2/MMT were present without UV light illumination, no As(V) were detected. When TiO_2/MMT were present with UV light illumination, a significant increase of As(V) concentration was observed in the first 20 min. This increase could be attributed to the continuous generation of As(V) from the photo-oxidation of As(III) by the photocatalytic TiO_2/MMT, which overrides the decrease of As(V) concentration by adsorption. With the increase of the illumination time, the As(V) concentration decreased from 34.0 to 1.2 $\mu g\,L^{-1}$, which largely decreases the As(V) concentration in the treated solution in spite of the continuous generation of As(V) by the photo-oxidation of As(III). Unlike some previous reports on photo-oxidation of As(III) in the TiO_2/UV system [10,38,39], the As(III) photo-oxidation to As(V) in our experiment is very low, far from near complete conversion. This difference is due to the excellent adsorption capability and fast adsorption rate of TiO_2/MMT on both As(III) and As(V).

The potential mechanisms of As(III) adsorption on TiO_2/MMT with UV irradiation were similar to the As(III) oxidation mechanisms in the TiO_2/UV system. TiO_2 can absorb UV light at less than 387.5 nm with energy greater than 3.2 eV, resulting in the promotion of an electron [e^-] into the conduction band (e_{cb}^-) and the formation of a positively charged hole [h^+] into the valence band (h_{vb}^+) (Reaction (R1)) [11]. A portion of the h_{vb}^+–e_{cb}^- pair escapes the recombination process and migrates to the TiO_2 surface, where it is converted to OH• and $O_2^{\bullet-}$ by reacting with OH^- and O_2, respectively (Reactions (R2) and (R3)).

$$TiO_2 \xrightarrow{h\nu} h_{vb}^+ + e_{cb}^- \quad \text{(R1)}$$

$$h_{vb}^+ + OH^- \rightarrow OH^\bullet \quad \text{(R2)}$$

$$e_{cb}^- + O_2 \rightarrow O_2^{\bullet-} \quad \text{(R3)}$$

$$As(III) \xrightarrow{h_{vb}^+} As(IV) \xrightarrow{OH^\bullet} As(V) \quad \text{(R4)}$$

As(III) may be oxidised to As(IV) by h_{vb}^+, OH• and $O_2^{\bullet-}$ in the TiO_2/UV system. However, which species plays a more important role is subject for debate. Lee and Choi [42] and Ryu and Choi [43] proposed $O_2^{\bullet-}$ as the major oxidant responsible for As(III) oxidation. However, Yoon and Lee [44] and Dutta et al. [45] reported that OH• is mainly responsible for the photocatalytic oxidation of As(III). In this study, constant N_2 flow was applied during As(III) adsorption and the deionised water was evaporated to remove O_2. However, the As(III) adsorption capacity increased with UV irradiation. These results suggest that OH• is the major oxidant responsible for As(III) adsorption on TiO_2/MMT with UV irradiation (Reaction (R4)). Work

Please cite this article in press as: Y. Li, et al., TiO_2 pillared montmorillonite as a photoactive adsorbent of arsenic under UV irradiation, Chem. Eng. J. (2012), doi:10.1016/j.cej.2012.02.058

Table 3
Comparison of adsorption capacity of arsenic on various adsorbents.

Sorbates	Adsorbents[a]	Initial concentration ($mg\,L^{-1}$)	Equilibrium concentration[b] ($mg\,L^{-1}$)	Equilibrium time (h)	pH	UV	Sorption capacity ($mg\,g^{-1}$)	Ref.
As(III)	Iron intercalated montmorillonite	2	0.310	12	5.5	Absent	4.4	[16]
	Nitrogen-doped titaniumoxide	1.02	0.069	1	7.5	Present	0.95	[35]
	Nanocrystalline titaniumdioxide	2	0.6	4	7	Present	8.3	[41]
	TiO_2-impregnated chitosan bead	10	7.79	185	6.6	Present	3.536	[32]
		10	8.68	185	9.2	Absent	2.099	
	Iron-impregnated chitosan	1	0.289	5	8	Absent	6.48	[30]
	Activated alumina	4.9	1	40	6.9	Absent	3.48	[8]
	Ce–Ti sorbent	–	0.01	12	6.5	Absent	7.5	[31]
	TiO_2/MMT	5	0	1.5	7	Present	5.19	This study
As(V)	Fe(III)-modified montmorillonite	4.17	4.092	6	6	Absent	3.07	[15]
	Nanocrystalline titaniumdioxide	2	0.15	4	7	Absent	11.2	[41]
	Iron intercalated montmorillonite	2	0.12	12	6.5	Absent	7.4	[16]
	TiO_2-impregnated chitosan bead	10	8.132	185	7	Present	2.988	[32]
		10	8.719	185	7.7	Absent	2.05	
	Activated alumina	11.52	0.1	170	5.2	Absent	15.9	[8]
	Ce–Ti sorbent	–	0.01	12	6.5	Absent	6.8	[31]
	TiO_2/MMT	5	0.004	2	7	Present	5.16	This study

[a] Powder adsorbent.
[b] Equilibrium concentration was calculated using the formula (1).

continues to further understand the arsenic adsorption mechanism on TiO_2/MMT with UV irradiation.

3.5. Arsenic adsorption by MMT, TiO_2, and TiO_2/MMT

For better understand the contribution and interaction of MMT and TiO_2 in the TiO_2/MMT composite, the adsorption capacity of TiO_2/MMT and an equivalent mass of its constituent components (84.9% MMT, 15.1%TiO_2) under various conditions were tested. Fig. 11 presents the arsenic adsorbed by TiO_2/MMT and the equivalent MMT and TiO_2 masses that compose the TiO_2/MMT in solutions with an initial Arsenic concentration (As(III) or As(V)) of 5.0 $mg\,L^{-1}$. As shown, only a small amount of As(III) and As(V) were removed by MMT, regardless of exposure to UV light. A pure TiO_2 adsorbent was also prepared in the presence of TiO_2/MMT using the hydrolysis method, and its adsorption capacity for As(III) was increased with UV irradiation. Whereas, the UV light had little effect on As(V) adsorption by pure TiO_2. By contrast, the arsenic adsorption capacities by adding the equivalent mass TiO_2 and MMT in arsenic aqueous were tested. Obviously, the TiO_2/MMT adsorbent had a much higher adsorption capacity than the pure TiO_2 and MMT adsorbents, indicating the synergistic effect of TiO_2 and MMT in the adsorption process.

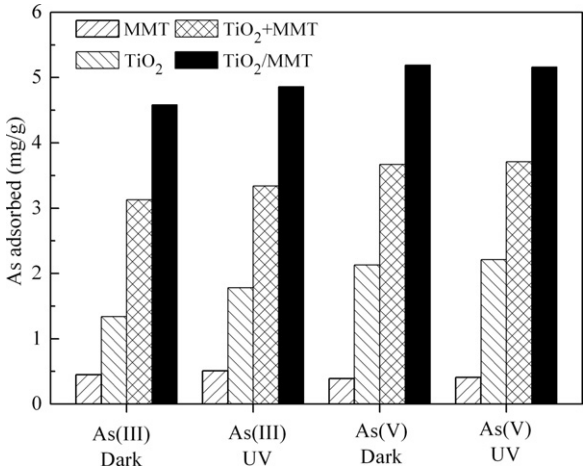

Fig. 11. Arsenic adsorbed by MMT, TiO_2 and TiO_2/MMT under various conditions, Adsorbent doses is equivalent to the mass present in 1.0 g TiO_2/MMT/L (i.e. 0.849 g MMT/L, 0.151 g TiO_2/L, (0.849 g MMT + 0.151 g TiO_2)/L, 1.0 g TiO_2/MMT/L).

Due to various differences in the experimental conditions, such as initial arsenic concentration, equilibrium concentration, pH and temperature, it is not possible to directly compare the adsorption efficiencies in various reports in the literature. Table 3 lists the adsorption capacity of As(III) and As(V) on the different adsorbents reported in the literature. Activated alumina is the most commonly used adsorbent for arsenic removal, but its adsorption capacity for As(III) is not satisfactory. Some iron-modified adsorbents, including iron-intercalated montmorillonite and iron-impregnated chitosan, have higher adsorption capacities for As(III) and As(V), but both need more time to reach equilibrium. Nanocrystalline titaniumdioxide has a higher adsorption capacity and faster adsorption rate for As(V), but it is difficult to remove TiO_2 from the finish water. Some TiO_2-based adsorbents such as the Ce–Ti adsorbent have higher adsorption capacities for arsenic at low equilibrium concentration, but they are expensive. Some natural adsorbents such as MMT are cheap, but their sorption capacities for arsenic are very low. Although the arsenic adsorption capacity on TiO_2/MMT is not the highest, the TiO_2/MMT adsorbent had a faster adsorption rate than comparable adsorbents and the equilibrium concentration of arsenic was lower than 10 $\mu g\,L^{-1}$ with UV irradiation.

3.6. Column study

In order to investigate the application of TiO_2/MMT to arsenic-contaminated groundwater adsorption, column adsorption of arsenic on granular TiO_2/MMT was conducted at different arsenic concentration. Fig. 12 presents the breakthrough curves of arsenic-contaminated groundwater at concentrations of 120 (As(III) 20%, As(V) 80%), 220 (As(III) 22.7%, As(V) 77.3%) and 410 $\mu g\,L^{-1}$ (As(III) 22%, As(V) 78%) when the arsenic solution at pH 8.0–8.2 was passed through the column at empty bed contact time (EBCT) of 2.0 min. The arsenic concentrations in the effluent were below the standard of 10 $\mu g\,L^{-1}$ (breakthrough point) at 4300, 5800 and 10,500 empty bed volumes (EBVs) with arsenic concentrations of 410, 220 and 120 $\mu g\,L^{-1}$, respectively. Gang et al. [30] conducted column tests using iron-chitosan composites for removal of As(III) at pH 8.0. Their results showed that the iron-chitosan composites could treat 796 EBVs with an As(III) concentration of 308 $\mu g\,L^{-1}$. Bang et al. [46] reported that approximately 10,000 EBVs of groundwater containing an average of 100 $\mu g\,L^{-1}$ of As(V) were treated by

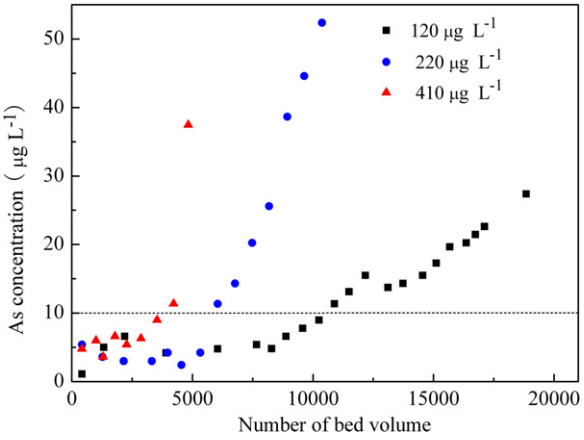

Fig. 12. The breakthrough curves of arsenic contaminated groundwater in the TiO_2/MMT adsorbent packed column.

granular TiO_2 at pH 7.1. Comparing EBVs between different studies is difficult due to column adsorption experiments using different adsorbents, column sizes, pH values and arsenic solutions.

4. Conclusion

In this study, after the replacement of the inactive sodium ions of montmorillonite with TiO_2, the TiO_2 pillared montmorillonite became highly active for arsenic removal. The XRD and XPS analyses indicated that TiO_2/MMT contained nanocrystalline titanium dioxide in the interlayer and on the external surface. These anatase TiO_2 nanoparticles were responsible for arsenic adsorption and photoactive adsorption. The arsenic adsorption experiments demonstrated that TiO_2/MMT can effectively remove arsenic from aqueous solutions under a wide range of experimental conditions, including pH, adsorption time and UV light. The equilibrium concentrations of As(III) and As(V) were less than 10 $\mu g L^{-1}$, especially with UV irradiation. The results from the adsorption kinetic experiments indicated that more than 90% and 87% of the As(III) and As(V) were absorbed by the TiO_2/MMT within the first 10 min with UV irradiation, respectively, and the adsorption kinetics fit the pseudo-second-order model well. The arsenic-contaminated groundwater removal column experiments indicated that columns packed with granular TiO_2/MMT could treat 10,500 bed volumes of an arsenic solution at a concentration of 120 $\mu g L^{-1}$ when the breakthrough point was 10 $\mu g L^{-1}$. The advantages of using TiO_2/MMT include its high efficiency for arsenic adsorption, faster adsorption rate, low equilibrium concentration of As(III) (0 $\mu g L^{-1}$) and As(V) (4 $\mu g L^{-1}$) with UV irradiation and low cost compared to the nanocrystalline titanium dioxide. Overall, the TiO_2/MMT adsorbent is a promising application for arsenic removal from arsenic-contaminated groundwater.

Acknowledgments

Financial support from the National Natural Science Foundation of China (Grant No. 20676094), the Science Foundation of Yunnan Province (No. 2006YX30) and the Social Development of Science and Technology Projects of Yunnan Province (No. 2009CA038) is gratefully acknowledged.

References

[1] D.K. Nordstrom, Worldwide occurrences of arsenic in ground water, Science 296 (2002) 2143–2145.
[2] U.K. Chowdhury, B.K. Biswas, T.R. Chowdhury, G. Samanta, B.K. Mandal, G.C. Basu, C.R. Chanda, D. Lodh, K.C. Saha, S.K. Mukherjee, S. Roy, S. Kabir, Q. Quamruzzamen, D. Chakraborti, Groundwater arsenic contamination in Bangladesh and West Bengal, India. Environ. Health Perspect. 108 (2000) 393–397.
[3] M.F. Hughes, Arsenic toxicity and potential mechanisms of action, Toxicol. Lett. 133 (2002) 1–16.
[4] A.H. Smith, P.A. Lopipero, M.N. Bates, C.M. Steinmaus, Arsenic epidemiology and drinking water standards, Science 296 (2002) 2145–2146.
[5] C.K. Jain, I. Ali, Arsenic: occurrence, toxicity and speciation techniques, Water Res. 34 (2000) 4304–4312.
[6] D. Mohan, C.U. Pittman, Arsenic removal from water/wastewater using adsorbents—a critical review, J. Hazard. Mater. 142 (2007) 1–53.
[7] S.M. Maliyekkal, L. Philip, T. Pradeep, As(III) removal from drinking water using manganese oxide-coated-alumina: performance evaluation and mechanistic details of surface binding, Chem. Eng. J. 153 (2009) 101–107.
[8] T.F. Lin, J.K. Wu, Adsorption of arsenite and arsenate within activated alumina grains: equilibrium and kinetics, Water Res. 35 (2001) 2049–2057.
[9] D. Nabi, I. Aslam, I.A. Qazi, Evaluation of the adsorption potential of titanium dioxide nanoparticles for arsenic removal, J. Environ. Sci. 21 (2009) 402–408.
[10] P.K. Dutta, A.K. Ray, V.K. Sharma, F.J. Millero, Adsorption of arsenate and arsenite on titanium dioxide suspensions, J. Colloid Interface Sci. 278 (2004) 270–275.
[11] M.A. Ferguson, M.R. Hoffmann, J.G. Hering, TiO_2 photocatalyzed As(III) oxidation in aqueous suspensions: reaction kinetics and effects of adsorption, Environ. Sci. Technol. 39 (2005) 1880–1886.
[12] H. Fei, W. Leng, X. Li, X. Cheng, Y. Xu, J. Zhang, C. Cao, Photocatalytic oxidation of arsenite over TiO_2: is superoxide the main oxidant in normal air-saturated aqueous solutions, Environ. Sci. Technol. 45 (2011) 4532–4539.
[13] M.P. Elizalde-Gonzalez, J. Mattusch, W.D. Einicke, R. Wennrich, Sorption on natural solids for arsenic removal, Chem. Eng. J. 81 (2010) 187–195.
[14] H.S. Altundogan, S. Altundogan, F. Tumen, M. Bildik, Arsenic removal from aqueous solutions by adsorption on red mud, Waste Manage. 20 (2000) 761–767.
[15] K.G. Bhattacharyya, S.S. Gupta, Adsorption of a few heavy metals on natural and modified kaolinite and montmorillonite: a review, Adv. Colloid Interface Sci. 140 (2008) 114–131.
[16] X.J. Ding, T.C. An, G.Y. Li, S.Q. Zhang, J.X. Chen, J.M. Yuan, H.J. Zhao, H. Chen, G.Y. Sheng, J.M. Fu, Preparation and characterization of hydrophobic TiO_2 pillared clay: the effect of acid hydrolysis catalyst and doped Pt amount on photocatalytic activity, J. Colloid Interface Sci. 320 (2008) 501–507.
[17] C. Ooka, S. Akita, Y. Ohashi, T. Horiuchi, K. Suzuki, S.I. Komai, H. Yoshida, T. Hattori, Crystallization of hydrothermally treated TiO_2 pillars in pillared montmorillonite for improvement of the photocatalytic activity, J. Mater. Chem. 9 (1999) 2943–2952.
[18] R. Kun, K. Mogyorosi, I. Dekany, Synthesis and structural and photocatalytic properties of TiO_2/montmorillonite nanocomposites, Appl. Clay Sci. 32 (2006) 99–110.
[19] C. Ooka, H. Yoshida, K. Suzuki, T. Hattori, Highly hydrophobic TiO_2 pillared clay for photocatalytic degradation of organic compounds in water, Micropor. Mesopor. Mater. 67 (2004) 143–150.
[20] X.J. Ding, T.C. An, G.Y. Li, J.X. Chen, G.Y. Sheng, J.M. Fu, H.J. Zhao, Photocatalytic degradation of dimethyl phthalate ester using novel hydrophobic TiO_2 pillared montmorillonite photocatalyst, Res. Chem. Intermed. 34 (2008) 67–83.
[21] C. Ooka, H. Yoshida, M. Horio, K. Suzuki, T. Hattori, Adsorptive and photocatalytic performance of TiO_2 pillared montmorillonite in degradation of endocrine disruptors having different hydrophobicity, Appl. Catal. B: Environ. 41 (2003) 313–321.
[22] G.K. Zhang, X.M. Ding, F.S. He, X.Y. Yu, J. Zhou, Y.J. Hu, J.W. Xie, Low-temperature synthesis and photocatalytic activity of TiO_2 pillared montmorillonite, Langmuir 24 (2008) 1026–1030.
[23] P. Na, X.M. Jia, B. Yuan, Y. Li, J.Y. Na, Y.C. Chen, L.S. Wang, Arsenic adsorption on Ti-pillared montmorillonite, J. Chem. Technol. Biotechnol. 85 (2010) 78–84.
[24] P.D. Christy, N.S.N. Jothi, N. Melikechi, P. Sagayaraj, Synthesis, structural and optical properties of well dispersed anatase TiO_2 nanoparticles by nonhydrothermal method, Cryst. Res. Technol. 44 (2009) 484–488.
[25] T. Ohno, K. Sarukawa, M. Masumura, Crystal faces of rutile and anatase TiO_2 particles and their roles in photocatalytic reactions, New J. Chem. 26 (2002) 1167–1170.
[26] N.N. Binitha, S. Sugunan, Preparation, characterization and catalytic activity of titanium pillared montmorillonite clays, Micropor. Mesopor. Mater. 93 (2006) 82–89.
[27] X. Tan, Q. Fan, X. Wang, B. Grambow, Eu(III) sorption to TiO_2 (anatase and rutile): batch, XPS, and EXAFS studies, Environ. Sci. Technol. 43 (2009) 3115–3124.
[28] P. Na, B.L. Zhao, L.Y. Gu, J. Liu, J.Y. Na, Deep desulfurization of model gasoline over photoirradiated titanium-pillared montmorillonite, J. Phys. Chem. Solids 70 (2009) 1465–1470.
[29] E.P. Barret, L.G. Joyner, P.P. Halenda, The determination of pore volume and area distributions in porous substances: I. Computations from nitrogen isotherms, J. Am. Chem. Soc. 73 (1951) 373–380.
[30] D.D. Gang, B.L. Deng, L.S. Lin, As(III) removal using an iron-impregnated chitosan sorbent, J. Hazard. Mater. 182 (2010) 151–161.
[31] Z. Li, S. Deng, G. Yu, J. Huang, V.C. Lim, As(V) and As(III) removal from water by a Ce–Ti oxide adsorbent: behavior and mechanism, Chem. Eng. J. 161 (2010) 106–113.
[32] S.M. Miller, J.B. Zimmerman, Novel, bio-based, photoactive arsenic sorbent: TiO_2-impregnated chitosan bead, Water Res. 44 (2010) 5722–5729.
[33] S. Goldberg, Competitive adsorption of arsenate and arsenite on oxides and clay minerals, Soil Sci. Soc. Am. J. 66 (2002) 413–421.

Please cite this article in press as: Y. Li, et al., TiO_2 pillared montmorillonite as a photoactive adsorbent of arsenic under UV irradiation, Chem. Eng. J. (2012), doi:10.1016/j.cej.2012.02.058

[34] S. Deng, Z. Li, J. Huang, G. Yu, Preparation, characterization and application of a Ce–Ti oxide adsorbent for enhanced removal of arsenate from water, J. Hazard. Mater. 179 (2010) 1014–1021.
[35] Q. Li, N.J. Easter, J.K. Shang, As(III) removal by palladium-modified nitrogen doped titanium oxide nanoparticle photocatalyst, Environ. Sci. Technol. 43 (2009) 1534–1539.
[36] Y.S. Ho, G. Mckay, Pseudo-second order model for sorption processes, Process Biochem. 34 (1999) 451–465.
[37] Y. Salameh, N. Al-Lagtah, M.N.M. Ahmad, S.J. Allen, G.M. Walker, Kinetic and thermodynamic investigations on arsenic adsorption onto dolomitic sorbents, Chem. Eng. J. 160 (2010) 440–446.
[38] M. Pena, X.G. Meng, G.P. Korfiatis, C.Y. Jian, Adsorption mechanism of arsenic on nanocrystalline titanium dioxide, Environ. Sci. Technol. 40 (2006) 1257–1262.
[39] F.S. Zhang, H. Itoh, Photocatalytic oxidation and removal of arsenite from water using slag-iron oxide-TiO_2 adsorbent, Chemosphere 65 (2006) 125–131.
[40] S. Chakraborty, M. Wolthers, D. Chatterjee, L. Charlet, Adsorption of arsenite and arsenate onto muscovite and biotite mica, J. Colloid Interface Sci. 309 (2007) 392–401.
[41] M.E. Pena, G.P. Korfiatis, M. Patel, L. Lippincott, X.G. Meng, Adsorption of As(V) and As(III) by nanocrystalline titaniumdioxide, Water Res. 39 (2005) 2327–2337.
[42] H. Lee, W. Choi, Photocatalytic oxidation of arsenite in TiO_2 suspension: kinetics and mechanisms, Environ. Sci. Technol. 36 (2002) 3872–3878.
[43] J. Ryu, W. Choi, Effects of TiO_2 surface modifications on photocatalytic oxidation of arsenite: the role of superoxides, Environ. Sci. Technol. 38 (2004) 2928–2933.
[44] S.H. Yoon, J.H. Lee, Oxidation mechanism of As(III) in the UV/TiO_2 system: evidence for a direct hole oxidation mechanism, Environ. Sci. Technol. 39 (2005) 9695–9701.
[45] P.K. Dutta, S.O. Pehkonen, V.K. Sharma, A.K. Ray, Photocatalytic oxidation of arsenic(III): evidence of hydroxyl radicals, Environ. Sci. Technol. 39 (2005) 1827–1834.
[46] S. Bang, M. Patel, L. Lippincott, X.G. Meng, Removal of arsenic from groundwater by granular titanium dioxide adsorbent, Chemosphere 60 (2005) 389–397.

Please cite this article in press as: Y. Li, et al., TiO_2 pillared montmorillonite as a photoactive adsorbent of arsenic under UV irradiation, Chem. Eng. J. (2012), doi:10.1016/j.cej.2012.02.058